SELF-HEALABLE AND MECHANICALLY STRONG HYDROGEL USING MODIFIED NANO-CELLULOSE CROSS LINKER

BY

SHYLA CHOWDHURY

STUDENT ID. 1018032714F

SESSION: OCTOBER 2018

MASTER OF SCIENCE IN CHEMISTRY

Soft and Smart Materials Research Group

Department of Chemistry

Bangladesh University of Engineering and Technology (BUET)

February 2021

Bangladesh University of Engineering and Technology
Department of Chemistry

The thesis entitled 'SELF-HEALABLE AND MECHANICALLY STRONG HYDROGEL USING MODIFIED NANO-CELLULOSE CROSS LINKER, submitted by Shyla Chowdhury, Roll No.: 1018032714F Session: October-2018, has been accepted as satisfactory in partial fulfillment of the requirement for the degree of Master of Science (M.Sc.) in Chemistry on 20.02.2021.

Board of examiners

1. Dr. Abu Bin Imran
   Associate Professor
   Department of Chemistry
   BUET, Dhaka.
   (Supervisor)

   Chairman

2. Head
   Department of Chemistry
   BUET, Dhaka.

   Member (ex-officio)

3. Dr. Al- Nakib Chowdhury
   Professor
   Department of Chemistry
   BUET, Dhaka.

   Member

4. Dr. Ayesha Sharmin
   Assistant Professor
   Department of Chemistry
   BUET, Dhaka.

   Member

5. Dr. Md. Mominul Islam
   Associate Professor
   Department of Chemistry
   University of Dhaka, Dhaka-1000

   Member (External)

Declaration by the candidate

I am hereby declared that this thesis or part of it has not been submitted elsewhere for award of any degree or diploma

……

Shyla Chowdhury

February 2021

Dedicated to

My Beloved Parents

Acknowledgement

First, I would like to express my gratitude to the Almighty Allah for his continuous blessing and mercy in giving a wonderful opportunity to carry out research at the most prestigious university in our country. I would like to express my warmest gratitude to our reverend supervisor Dr. Abu Bin Imran, associate professor, Department of Chemistry (BUET), for his endless support, encouragement, and guidance throughout the journey. I sincerely thank him for his kindness, positive outlook, and immense generosity. I believe I am the luckiest person to get the opportunity to be part of his research team and be supervised by him. I would like to express my heartfelt gratitude and respect to Dr. Al-Nakib Chowdhury, Professor and Head of the Department of Chemistry (BUET), for his guidance and valuable advice. I also like to convey my deepest gratitude to my respected teacher Professor Dr. Md. Shakhawat Hossain Firoz, honorable Professor the Department of Chemistry (BUET), for giving me excellent advice and inspiration in my academic career. I would also like to sincerely thank Dr. Ayesha Sharmin, Dr. Chanchal Kumar Roy, and Dr. Md. Ayub Ali for their insightful advice and guidance during the academic period. I am also sincerely expressing my gratitude towards all my respected faculty of the Department of Chemistry (BUET), for their advice and inspiration. My special thanks to all the department staff for helping me during this research. I am truly grateful to the Department of Glass and Ceramics (BUET), for assisting me during characterization procedures such as FE-SEM and EDX. Finally, my heartfelt thanks and gratitude towards all the members of Soft and Smart Materials Research Group for assisting me in every possible way. I cannot forget the help from Sarmin Akter, Noman Chowdhury, Md Rezaul Karim, Md. Aminul Rahman, Md. Amjad Hossain, Md. Mosfeq Uddin and H. B. Muhammad Zukaul Islam. I would like to give my heartful thanks to them.

Shyla Chowdhury

February 2021

Abstract

Hydrogels with mechanical strength and self-healing properties can mimic characteristics of biological load-bearing soft tissues. Thus, they have drawn attention over the past few years. However, it is quite challenging to incorporate both properties simultaneously into the hydrogels. Developing strategies to fabricate mechanically robust and self-healable hydrogels is yet to be realized. In this work, we developed a one-pot method to prepare nontoxic, environmentally friendly hydrogel via free radical polymerization using a modified nano-cellulose cross-linker, natural polymer Alginic acid and $FeCl_3.6H_2O$. Here, nano-cellulose cross-linker was derived from micro-crystalline cellulose and then chemically functionalized with a traditional silane coupling agent to introduce a large number of carboxyl groups on the backbone chain of the polymer network. By using Ferric ions, we tried to introduce reversible and dynamic metal coordination bond, which has been proved to improve mechanical and self-healing properties of hydrogels. Dual metal coordination bonds with dynamic features will serve as sacrificial bonds leading to the effective self-healing efficiency after damage. The mechanical toughness of prepared hydrogel was analyzed by universal testing machine and the spectroscopic analysis and rheological measurements corroborated the existence of hydrogen and dual coordination bonds. Finally, the fabricated hydrogels showed excellent self-healing property, which was highly stretchable after damaging without applying external stimulation such as pH or temperature. It is expected that the synthesized hydrogel with high mechanical properties and time-dependent self-healing ability may diversify its practical applications in biomedical fields.

Contents

Figures

List of tables

List of Abbreviations of Technical Symbols and Terms

1. Acrylic Acid (AA)
2. 3-(Trimethoxysilyl) propyl methacrylate (MPTS)
3. Nano crystalline cellulose (NCC)
4. Modified nano crystalline cellulose (MNCC)
5. Tetramethylethylenediamine (TEMED)
6. Alginic acid (Alg)

Chapter 1

Introduction

1.1 Introduction

Hydrogels are essential functional materials known for their three-dimensional cross-linked hydrophilic networks capable of retaining large amounts of water without dissolving [1-3]. They are soft materials formed through the self-assembly of polymers, creating either covalently or physically cross-linked networks [4-6]. Thanks to their unique properties, such as high hydrophilicity, permeability, and biocompatibility, hydrogels share similarities with biological tissues [7]. As a result, they have been widely used as scaffolds, drug delivery vehicles, models for extracellular matrices in cell culture, and tissue engineering applications [8-10]. Despite their various applications, most hydrogels suffer from poor mechanical strength and low deformation capacity [11]. This limitation hinders their high-end use, particularly in load-bearing soft tissues like ligaments, cartilage, and tendons, which require stiffness, toughness, fatigue resistance, and self-healing properties [12-14]. The fragility of hydrogels primarily arises from the random arrangement of cross-linkers [15], necessitating a secondary interaction mechanism to reinforce the primary network. One way to achieve this is by introducing chemical bonding for additional strength [16]. However, chemical bonding tends to be irreversible, and stress concentration during loading can lead to damages, significantly reducing mechanical performance during repeated loadings. To address these challenges, researchers have sought to incorporate non-chemical interactions, such as hydrogen or metal coordination bonds [17-18]. These non-covalent bonds can break and reform reversibly, leading to enhanced mechanical strength in hydrogels [19]. The covalent bonds provide permanent crosslinks that maintain the integrity of the hydrogel, while the non-covalent bonds act as sacrificial bonds, contributing to the improved mechanical properties. One example of a dynamic non-covalent interaction is the metal-ligand coordination bond, which offers a wide spectrum of bonding strength, resulting in increased toughness and stiffness [27-29]. By combining physical crosslinking with the migration of ferric ions, researchers have achieved self-healing capacity in hydrogels [30]. For instance, the incorporation of COOH-Fe^{3+}metal-ligand interactions into poly (acrylamide-co-

acrylic acid) hydrogels have further strengthened their mechanical properties [31]. Moreover, nano-crystalline cellulose (NCC) and natural polymer Alginic acid, with their native crystalline structures, have gained attention as environmentally friendly reinforcing particles due to their modifiability, biocompatibility, renewability, biodegradability, and excellent mechanical integrity [32]. The introduction of vinyl groups in NCC, achieved through modification with 3-methacryloxypropyltrimethoxysilane (MPTS), allows for the formation of covalent bonds, serving as sacrificial bonds in a transient network to investigate the energy dissipation mechanism. This approach successfully enhances the mechanical properties of hydrogels and introduces self-healing abilities to them.

In summary, combining physically and chemically cross-linked networks in hydrogels offers a promising strategy to integrate self-healing properties and improved mechanical performance. By leveraging dynamic non-covalent interactions alongside strong chemical bonding, researchers are making strides in overcoming the limitations of hydrogels and unlocking their potential in various applications.

1.2 Objectives:

The main objective of this work is to

- Synthesize of a nontoxic nano-cellulose cross-linker.
- Fabrication of a biodegradable and eco-friendly mechanically strong hydrogel using the synthesized cross-linker.
- To incorporate self-healing properties into the mechanically strong hydrogel.
- Establishing the superior mechanical properties of the synthesized hydrogels.

1.3 Background

1.3.1 Hydrogels

Hydrogels are networks of three-dimensional hydrophilic polymer chains that can store a lot of water and have characteristics similar to solids and liquids [33]. Individual polymer chains are cross-linked chemically or physically to retain the structure of the

Hydrogels [34]. The discovery of hydrogels was first made by Wichterle and Lam in 1960 [35].For a substance to be considered a hydrogel, water must make up at least 10% of the total weight (or volume) [36]. Due to their high-water content, it shows similarity to biological tissues by having a degree of flexibility. The hydrophilic groups -NH_2, -COOH, -OH, -$CONH_2$, -CONH -, and -SO_3H give the polymer network its hydrophilicity [37-38]. For this, several cross-linkers, including 1,4-butanediol diacrylate (BDDA), N, N-cysteinebisacrylamide (CBA), and N, N-methylenebisacrylamide (BIS), are utilized [39]. They have a wide range of applications, including medication delivery systems, sensors, actuators, and biomaterials. Nevertheless, the hydrogel's practical uses are frequently hindered because of their poor mechanical properties such as being too weak or brittle, low toughness, low stretching and bending ability, and low elastic modulus. [40-41]. Recently some steps have already been taken to overcome these limitations. Figure 1.1 below provides a visual illustration of a hydrogel.

Fig. 1. 1 Picture of the synthesized hydrogel

1.3.2 Different types of hydrogel

Classifications of hydrogels could be made by various ways such as,

1.3.2.1 Types of hydrogels based on crosslinking

According to how they are cross-linked, hydrogels may be divided into two groups: (a) Physically cross-linked hydrogels and (b) Chemically cross-linked hydrogels [42–43].

1.3.2.2 Hydrogels based on physical crosslinking

Physically cross-linked hydrogels are created by ionic contact, crystallization, stereo complex creation, hydrophobized polysaccharides, protein interaction, and hydrogen bonding [44]. Due to their relative simplicity of manufacture and the benefit of not requiring crosslinking chemicals during their synthesis technique, physically cross-li nked hydrogels have attracted much interest [45]. Here is a discussion of the numerous methods for producing physically cross-linked hydrogels. This category includes ionic polymers cross-linked in hydrogel systems using di- or trivalent counter ions. The idea behind gelling a polyelectrolyte solution with multivalent ions of the opposite charge is based on this technique [46]. Chitosan-glycerol phosphate salt hydrogels are an example of hydrogels that fall under this group. Hydrogen bonding interactions can be used to create physically cross-linked gel-like structures. Developing a hydrogen-bond carboxymethylcellulose (CMC) network by dispersing CMC in 0.1 M HCl is the most outstanding illustration of such a hydrogel [47]. In this procedure, hydrogen from the acid replaces the sodium ions in the CMC.

1.3.2.3 Hydrogels based on chemically crosslinking

Covalent bonds connect different polymer chains in chemically cross-linked hydrogels. As a result, they are stable and cannot dissolve in any solvents without cleaving the covalent crosslinks. A physically cross-linked hydrogel's design flexibility is constrained since it is challenging to decouple factors such as gelation time, internal network pore size, chemical functionalization, and degradation time [48]. On the other hand, chemical crosslinking produces a network with a reasonably high mechanical strength depending on the kind of chemical bonds in the building blocks and the crosslinks.

1.3.3 Hydrogel's Responsiveness

Temperature, pH, electric field, light, magnetic field, and other stimuli are common stimuli. Dissolution precipitation, degradation, drug release, change in hydration state, swelling or collapsing, hydrophilic or hydrophobic surface, shape change, and conformational change are all possible responses. Many studies have shown that combining MCC and other polymers results in pH-sensitive hydrogels with noticeable mechanical strength [49]. Cross-linked, hydrophilic polymer networks called stimulus-responsive hydrogels change physiochemically in reaction to external stimuli, including pH, temperature, light, and analyte concentration.

1.3.4 Swelling properties of hydrogel

When water or a solvent is introduced to a cross-linked polymer hydrogel, it undergoes expansion without dissolving. The liquid medium acts as a selective filter, allowing some solute molecules to freely diffuse while the polymer network acts as a matrix, holding the liquid within its structure. The extent of swelling is influenced by several factors, including the density of the network, the nature of the solvent, and the interaction parameters between the polymer and the solvent. In a hydrophilic polymer network, water serves as a plasticizer. When a dry hydrogel absorbs water, the first water molecules hydrate the most polar and hydrophilic groups in the matrix, forming primary bonded water. As these polar groups become hydrated, the network swells, exposing hydrophobic groups that then interact with water molecules, resulting in hydrophobically-bound water, also known as secondary bound water. This dual mechanism of water interaction contributes to the overall swelling behavior of the hydrogel.

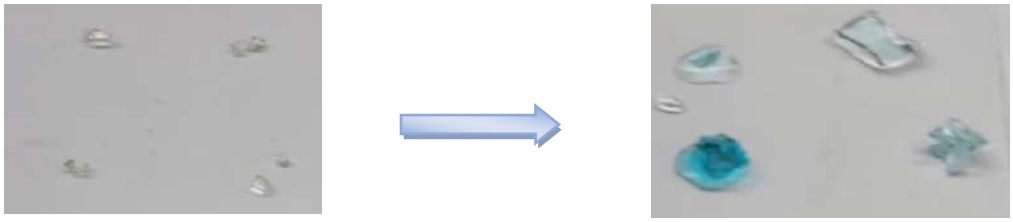

Figure 1.2 Water swelling by hydrogel

The covalent or physical crosslink opposes this additional swelling, resulting in an elastic network retardation force. As a result, the hydrogel will achieve an equilibrium level of swelling. When the ionic, polar, and hydrophobic groups have become saturated with bound water the additional water that is inserted is referred to as free water or bulk water, and it is considered to occupy the space between the network chains, as well as the center of larger pores, macropores, or voids. The network chains or crosslinks are assumed to be degradable if the gel begins to disintegrate and dissolve as the network swells.

1.3.5 Mechanical properties

The mechanical properties of a material can be varied and regulated depending on its intended use. It is expected to obtain a stiffer gel by increasing or decreasing the crosslinking degree. Different causes and variables of polymeric materials are responsible for changing the mechanical properties. It is worthy of mention that in a hydrogel, tensile strength is essential for a material that will be stretched or under tension. Young's Modulus is the result of how water and gel matrices combine together. Toughness is the quality of being strong under high stress and not easily broken. Whereas, ductility is the ability to be plastically deformed without fracture or torn out. The property of ductility is gathered from the value of elongation at break in percent.

1.3.6 Polymerization condition

The reaction conditions have a significant impact on the final polymer product. Factors with regard to which the polymerization reactions are influenced are the amount of monomer, reinforcement agent, reaction time, temperature, and type of solvent. The type and quantity of solvent utilized during polymerization are very crucial. If the solvent part is used in a large ratio during the polymerization, cycles will form rather than crosslinks with the crosslinking agent. The effective crosslink density will be reduced due to this alteration, lowering the material strength. The copolymer structure may change when the criteria of the solvent (for instance, pH or ionic strength) are modified. Because ionic strength and pH have varying effects on monomer reactivity. These conditions alteration could transform the copolymer from random to block or create significant changes in the copolymer composition. The structure and nature of the polymer formed in a large amount of solvent significantly differ from the polymer formed in bulk polymerization. The functional group conversion can be adjusted using the abovementioned factors. If, without any post-reaction treatments hydrogels are processed, the double bond conversion enhancement can lead to drastically improved mechanical properties [50]. Changes in network structure and material strength can also be achieved with post-reaction treatments.

1.3.7 Adsorption capacity of hydrogels

Leading environmental pollutants that require emergency attention include heavy metals, persistent organic pollutants, synthetic colors, and industrial wastewater. Hydrogels have lately been studied for wastewater treatment. The functional groups of these polymeric networks can be changed, resulting in a high binding affinity for various pollutants in wastewater.

In this article, many forms and variations of hydrogels, with a focus on the adsorption capability of model dyes will be discussed targeting to treat dyeing industrial effluents. In addition, the adsorption process, kinetics, pH dependency, isotherm, and related thermodynamic characteristics of the modified hydrogels have been studied using a comparative method.

1.4 Applications of Hydrogel

1.4.1 Drug delivery applications

Polymeric hydrogels have been a subject of great interest since the 1950s. Their unique properties, such as external trigger responsiveness and spatiotemporal release mechanisms, make them promising candidates for various physiological applications, including cancer treatment, osteoarthritis, diabetes, managing viral and bacterial infections, addressing cardiac illnesses, and more [51, 52]. One of the key advantages of using hydrogels in drug delivery is their ability to facilitate controlled and sustained release of pharmaceutical components, leading to longer-lasting effects [53]. Hydrogels excel in drug delivery applications due to their exceptional water-absorption capacity, being capable of absorbing more than 90% of their weight in water. This outstanding hydrophilic property sets them apart from other drug delivery methods, allowing for regulated diffusion rates and efficient encapsulation and controlled release of active pharmaceutical agents. The ability to provide extended drug release over time

makes them a valuable tool in the realm of therapeutic treatments.

1.4.2 Hydrogel in Tissue Engineering Tissue engineering

Research and development seek to combine principles from cell biology and engineering to develop biological substitutes capable of repairing, preserving, or enhancing the shape and function of damaged tissues and organs [54]. A fundamental aspect of tissue engineering is creating biocompatible and biodegradable cell scaffolds, and hydrogels represent a significant class of materials that fulfill this role [55]. Hydrogels are widely used as scaffold materials in tissue engineering for several compelling reasons. Firstly, they share similarities with soft tissues, being flexible and soft in their natural environment. Secondly, when liquid hydrogels are injected into the body, they quickly fill tissue defects, solidifying into irregular, nonflowing semisolids [56]. This feature facilitates efficient and precise filling of tissue voids. Lastly, by tuning the porosity and pore size while expanding the internal surface area, hydrogels can create a three-dimensional polymeric network structure that mimics the natural extracellular matrix, providing an ideal environment for cell engraftment, adhesion, and proliferation [57]. This enables the growth of new tissue and promotes the integration of the scaffold with the surrounding biological tissues.

1.5 References

[1] Nam, C., Zimudzi, T. J., Geise, G. M., Hickner, M. A. Increased Hydrogel Swelling Induced by Absorption of Small Molecules. ACS Appl. Mater. Interfaces vol.8, pp. 14263−14270, 2016.

[2] Du, X., Zhou, J., Shi, J., Xu, B. Supramolecular Hydrogelators and Hydrogels: From Soft Matter to Molecular Biomaterials. Chem. Rev. vol. 115, pp. 13165−13307, 2015.

[3] M. J., Webber, Appel, E. A., Meijer, E., Langer, R. Supramolecular Biomaterials. Nat.Mater.vol.15, pp.13−26, 2016.

[4] K. Y. Lee and D. J. Mooney, Chem. Rev, vol. 101, pp. 1869, 2001.

[5] J. L. Drury and D. J. Mooney, Biomaterials, vol. 24, pp. 4337, 2003.

[6] J. J. Schmidt, J. Rowley and H. J. Kong, J. Biomed. Mater. Res, Part A, vol. 87, pp. 1113, 2008.

[7] Shao, C. Chang, H., Wang, M. Xu, F.Yang, J. High-Strength, Tough, Self-Healing Nanocomposite Physical Hydrogels Based on the Synergistic Effects of Dynamic Hydrogen Bond and Dual Coordination Bonds. ACS Appl. Mater. Interfaces, vol.9, pp. 28305-28318, 2017.

[8] Lee, K. Y., Mooney, D. J. Hydrogels for Tissue Engineering. Chem. Rev. 101, pp.1869−1880, 2001.

[9] Secret, E., Kelly, S. J., Crannell, K. E.; Andrew, J. S. Enzyme Responsive Hydrogel Micro particles for Pulmonary Drug Delivery. ACS Appl. Mater. Interfaces, vol. 6, pp. 10313−10321, 2015.

[10] Zhao, X. Multi-Scale Multi-Mechanism Design of Tough Hydrogels: Building Dissipation into Stretchy Networks. Soft Matter, vol.10, pp. 672−687, 2014.

[11] Discher, D. E.; Mooney, D. J.; Zandstra, P. W. Growth Factors, Matrices, and Forces Combine and Control Stem Cells. Science, vol. 324, pp. 1673−1677, 2009.

[12] Seliktar, D. Designing Cell-Compatible Hydrogels for Biomedical Applications. Science, vol.336, pp. 1124−1128, 2012.

[13] Wang, Q., Mynar, J. L., Yoshida, M., Lee, E., Lee, M., Okuro,K., Kinbara, K., Aida, T. High-Water-Content Mouldable Hydrogels by Mixing Clay and a Dendritic Molecular Binder. Nature, vol. 463, pp. 339−343, 2010.

[14] Y, Takashima,., Hatanaka, S., Otsubo, M., Nakahata, M., Kakuta,T., Hashidzume, A., Yamaguchi, H., Harada, A. Expansion− Contraction of Photoresponsive Artificial Muscle Regulated by Host−guest Interactions. Nat. Common.,vol. 3, pp. 1270−1278, 2010.

[15] Ye, L., Tang. Y., Qiu, D. Enhance the mechanical performance ofpolyacrylamide hydrogel by aluminium-modified colloidal silica, Colloids and Surfaces A, vol. 447, pp.103-110, 2014.

[16] Y. Okumura, K. Ito, The polyrotaxane gel: a topological gel by figure-of-crosslinks, Adv.Mater.vol. 13, pp. 485–487, 2011.

[17] Y.H. Na, Y. Tanaka, Y. Kawauchi, H. Furukawa, T. Sumiyoshi, J.P. Gong, Y. Osada, Necking phenomenon of double-network gels, Macromolecules, vol.39, pp. 4641–4644, 2006.

[18] R.E. Webber, C. Creton, H.R. Brown, J.P. Gong, Large strain hysteresis and Mullins effect of tough double-network hydrogels, Macromolecules vol.40, pp. 2919–2927, 2007.

[19] Gong, J. P. Why Are Double Network Hydrogels So Tough? Soft Matter, vol. 6, pp. 2583−2590, 2010.

[20] Haque, M. A., Kurokawa, T., Kamita, G., Gong, J. P. Lamellar Bilayers as Reversible Sacrificial Bonds to Toughen Hydrogel: Hysteresis, Self-Recovery, Fatigue Resistance, and Crack Blunting. Macromolecules, vol.44, pp. 8916−8924, 2011.

[21] Sun, J. Y., Zhao, X., Illeperuma, W. R. K., Chaudhuri, O., Oh, K.H., Mooney, D. J., Vlassak, J. J., Suo, Z. Highly Stretchable and Tough Hydrogels.Nature,vol 489, 133−136, 2011.

[22] Zheng, S., Ding, H., Qian, J., Yin, J., Wu, Z. L., Song, Y., Zheng, Q. Metal-Coordination Complexes Mediated Physical Hydrogels with High Toughness, Stick−Slip Tearing Behavior, and Good Process ability. Macromolecules, vol. 49, pp.9637−9646, 2016.

[23] Henderson, K. J., Zhou, T. C., Otim, K. J., Shull, K. R. Ionically Crosslinked Triblock Copolymer Hydrogels with High Strength. Macromolecules, vol .43, pp. 6193−6201, 2010.

[24] Chen, Q., Zhu, L., Chen, H.,Yan, H. L., Huang, L. N., Yang, J., Zheng, J. A Novel Design Strategy for Fully Physically Linked Double Network Hydrogels with Tough, Fatigue Resistant, and Self-Healing Properties. Adv. Funct. Mater. Vol. 25, pp. 1598−1607, 2015.

[25] Rybtchinski, B. Adaptive Supramolecular Nanomaterials Based on Strong Noncovalent Interactions. ACS Nano, vol. 5, pp. 6791−6818, 2011.

[26] Herbst, F., Döhler, D., Michael, P., Binder, W. H. Self-Healing Polymers via Supramolecular Forces. Macromol. Rapid Commun, vol. 34, pp. 203−220, 2013.

[27] Lee, B. P., Konst, S. Novel Hydrogel Actuator Inspired by Reversible Mussel Adhesive Protein Chemistry. Adv. Mater, vol. 26, pp. 3415−3419, 2014.

[28] Hu, Y., Du, Z., Deng, X., Wang, T., Yang, Z., Zhou, W.,Wang, C. Dual Physically Cross-Linked Hydrogels with High Stretchability, Toughness, and Good Self-Recoverability.Macromolecules, vol. 49, pp. 5660−5668, 2016.

[29] Chen, Q., Yan, X., Zhu, L., Chen, H., Jiang, B., Wei, D., Huang, L., Yang, J., Liu, B., Zheng. Improvement of Mechanical Strength and Fatigue Resistance of Double Network Hydrogels by Ionic Coordination Interactions. Chem. Mater, vol. 28, pp. 5710−5720, 2016.

[30] Wei, Z., He, J., Liang, T., Oh, H., Athas, J., Tong, Z., Wang, C., Nie, Z. Autonomous Self-Healing of Poly (acrylic acid) Hydrogels Induced by the Migration of Ferric Ions. Polym.Chem, vol. 4, pp. 4601− 4605, 2013.

[31] Lin, P., Ma, S., Wang, X., Zhou, F. Molecularly Engineered Dual-Crosslinked Hydrogel with Ultrahigh Mechanical Strength, Toughness, and Good Self-Recovery. Adv. Mater, vol. 27, pp. 2054− 2059, 2015.

[32] Payen, A. Compt. Rend., vol. 7, pp. 1052, 1838.

[33] L. Ye, Y. Tang, and D. Qiu, 'Enhance the mechanical performance of olyacrylamide hydrogel by aluminium-modified colloidal silicanhan,' Colloids Surfaces a Physicochem. Eng. Asp. vol. 447, pp. 10," Colloids Surfaces A Physicochem. Eng. Asp, vol. 447, pp. 103–110, 2014.

[34] J. Maitra and V. K. Shukla, "Crosslinking in Hydrogel - A Review," Am. J. Polym. Sci., vol. 25, pp. 2163-1342, 2014.

[35] Wichterle, O. and Lim, D. "Hydrophilic Gels for Biological Use, “Nature, vol.185, pp. 117-118, (1960). M. B. Mellott, K. Searcy, and M. V.Pishko,"Releaseof protein from highly cross-linked hydrogels of poly (ethylene glycol)diacrylate fabricated by UV polymerization," Biomaterials. 22, pp. 929-941, 2001.

[36] X. Zhang, G. Lin, S. R. Kumar, and J. E. Mark, "Hydrogels prepared from polysiloxane chains by end linking them with trifunctional silanes containing hydrophilic groups," Polymer (Guildf)., vol. 50, pp. 5414–5421, 2009.

[37] R. Guo, Q. Su, J. Zhang, A. Dong, C. Lin, and J. Zhang, "Facile Access to Multisensitive and Self-Healing Hydrogels with Reversible and Dynamic Boronic Ester and Disulfide Linkages," Biomacromolecules, vol. 18, pp.1356−1364, 2017.

[38] F. Rossi, G. Perale, G. Storti, and M. Masi, "A library of tunable agarose carbomer-based hydrogels for tissue engineering applications: The role of

cross-linkers," J. Appl. Polym. Sci., vol.123, pp. 2211-2221, 2012.

[39] S. Deshmukh, D. A. Mooney, and J. M. D. MacElroy, "Molecular simulation study of the effect of cross-linker on the properties of poly (N-isopropyl acrylamide) hydrogel," Mol. Simul., vol. 37, pp.846-854, 2011.

[40] S. Liu et al., "Polysaccharide-templated preparation of mechanically-tough, conductive and self-healing hydrogels," Chem. Eng. J., vol.334, pp. 2220-2230, 2018.

[41] Bilotti, E. and Mary, Q., "Polymer/Sepiolite Clay Nanocomposites," PhD. thesis, School of Engineering and Materials Science, University of London, 2009.

[42] S. Van Vlierberghe, P. Dubruel, and E. Schacht, "Biopolymer-based hydrogels as scaffolds for tissue engineering applications: A review," Biomacromolecules. vol. 12, pp.1287-1408, 2011.

[43] E. Caló and V. V. Khutoryanskiy, "Biomedical applications of hydrogels: A review of patents and commercial products," European Polymer Journal.vol. 65, pp. 252-267, 2015.

[44] K. Shaini, "Preparation method, Properties and Crosslinking of hydrogel: a review," PharmaTutor, vol. 5, pp. 27-36, 2017.

[45] M. F. Akhtar, M. Hanif, and N. M. Ranjha, "Methods of synthesis of hydrogels A review," Saudi Pharmaceutical Journal. Vol. 24, pp. 554-559, 2016.

[46] N. Bhattarai, J. Gunn, and M. Zhang, "Chitosan-based hydrogels for controlled, localized drug delivery.," Adv. Drug Deliv. Rev., vol. 62 pp.83-99, 2010.

[47] Baker. J. P., Blanch, H. W. and Prausnitz, J. M., "Equilibrium swelling properties of weakly ionizable 2-hydroxyethyl methacrylate (HEMA)-based hydrogels", Journal of Applied Polymer Science, Vol. 52, pp. 783-788, 1994.

[48] Vasi, A. M., Popa, M. I., Tanase, E. C., Butnaru, M. and Verestiuc, L., "Poly (acrylic acid)-poly (ethylene glycol) nanoparticles designed for ophthalmic drug delivery", Journal Pharmaceuticals Science, Vol. 103, pp. 676-686, 2014.

[49] Baker. J. P., Blanch, H. W. and Prausnitz, J. M., "Equilibrium swelling properties of weakly ionizable 2-hydroxyethyl methacrylate (HEMA)-based hydrogels", Journal of Applied Polymer Science, Vol. 52, pp. 783-788, 1994.

[50] Bao Y, Ma J, Li N., "Synthesis and swelling behaviors of sodium carboxymethyl cellulose-poly (AA-co-AM-co-AMPS)/MMT superabsorbent hydrogel", Carbohydrate Polymer, Vol. 84, pp. 76–82, 2011.

[51] R. M. Wang and K. L. Christman, "Decellularized myocardial matrix hydrogels: In basic research and preclinical studies," Advanced Drug Delivery Reviews. vol.15 pp.77-82, 2016.

[52] M. Hamidi, K. Rostamizadeh, and M. A. Shahbazi, "Hydrogel Nanoparticles in Drug Delivery," in Intelligent Nanomaterials: Processes, Properties, and Applications, vol.5 pp.583-624, 2012.

[53] M. R. Guilherme et al., "Superabsorbent hydrogels based on polysaccharides for application in agriculture as soil conditioner and nutrient carrier: A review," European Polymer Journal.vol.72, pp. 365-385, 2015.

[54] T. Billiet, M. Vandenhaute, J. Schelfhout, S. Van Vlierberghe, and P. Dubruel, "A review of trends and limitations in International Journal of Polymer Science 13 hydrogel-rapid prototyping for tissue engineering," Biomaterials, vol. 33, no. 26, pp. 6020–6041, 2012.

[55] P. Matricardi, C. Di Meo, T. Coviello, W. E. Hennink, and F. Alhaique, "Interpenetrating polymer networks polysaccharide hydrogels for drug delivery and tissue engineering," Advanced drug delivery reviews, vol. 65, no. 9, pp. 1172– 1187, 2013.

[56] H. K. Cheung, T. T. Y. Han, D. M. Marecak, J. F. Watkins, B. G. Amsden, and L.

[57] H. Park, B. Choi, J. Hu, and M. Lee, "Injectable chitosan hyaluronic acid hydrogels for cartilage tissue engineering," Acta Biomaterialia, vol. 9, no. 1, pp. 4779–4786, 2013.

Chapter 2

Experimental

2.1 Instruments and materials

2.1.1 Reagents and Chemicals

- Acrylic acid (AA)(Sigma Aldrich Chemical Co.) 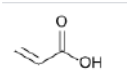
- 3-Methacryloxypropyltrimethoxysilane (MPTS) 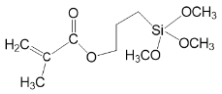
- Alginic acid 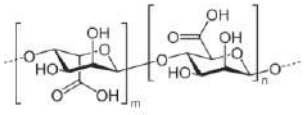
- Ferric Chloride Hexahydrate ($FeCl_3.6H_2O$)
- Sulfuric acid (Merck, Germany)
- Acetic acid (CH_3COOH) 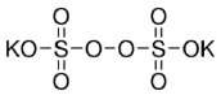
- Potassium persulfate (KPS) (BDH)
- Ethanol (CH_3CH_2OH) (Merck, Germany)
- Tetramethylethylenediamine (TEMED)
- Microcrystalline Cellulose (MCC) (Sigma-Aldrich)
- Deionized water

2.1.2 Instrument

Analysis of the samples was performed using the following instruments:

• Centrifuge machine (Hettich, Universal 16A)

• pH meter (Hanna, HI 8424, Romania)

• Digital Balance (AB 265/S/SACT METTLER, Toleto, Switzerland)

• Freeze dryer (Heto FD3)

• Oven dryer (Lab Tech, LDO-030E, Korea)

• Fourier Transform Infrared Spectrophotometer (SHIMADZU FTIR-8400)

• Universal testing machine (Test resources, 100P250-12 System, USA)

• Orbital Shaker

• UV–Vis spectrophotometer (SHIMADZU UV- 1601)

2.2Method of Preparation

2.2.1Procedureto prepare NCC through H_2SO_4 hydrolysis:

In a 500 mL round bottom flask, 10g of microcrystalline cellulose was added with 200 mL 63.4% (w/w) [1-3] H_2SO_4. The mixture and a magnetic stirrer were placed in an oil bath at 60°C temperature for 1 hour. Cellulose and H_2SO_4 mixture was hydrolyzed with continuous stirring. After 90 minutes, the flask was placed in an ice bath for cooling. The ultra-sonication was applied for 15 minutes. The mixture was then allowed to settle until the top layer was transparent and was washed with distilled water several times until the mixture turned into a white suspension. To eliminate extra acid and water-soluble particles, the suspension was put into a centrifuge tube and agitated at 4000 rpm for 10 minutes. After that, deionized water was used to wash the cellulose suspension. To decrease the acid content, the procedure was repeated multiple times. The suspension was then freeze-dried and NCC was obtained in powdered form.

2.2.2 Visual representation of preparing NCC through H_2SO_4Hydrolysis:

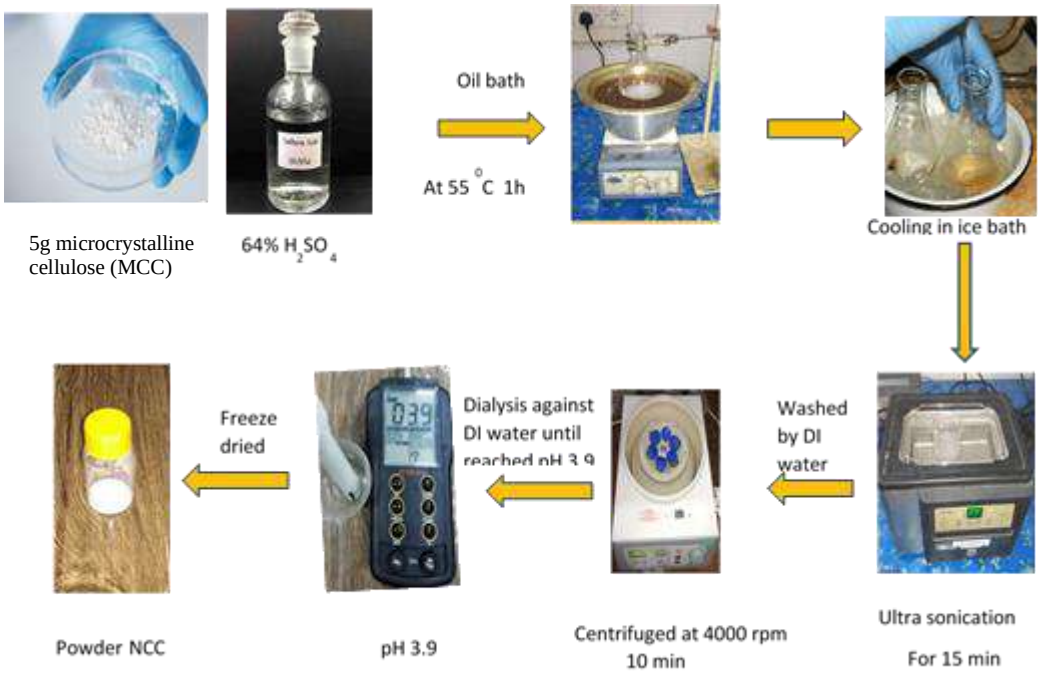

Fig. 2. 1 Synthesis diagram of Nano Crystalline Cellulose (NCC)

2.2.3 Preparation of modified nano crystalline cellulose (MNCC)

At the beginning of this procedure, ethanol and water (9:1 vol %) were poured into a round bottom flask. MPTS (10% w/w of NCC) was added carefully into this mixture to hydrolyze adequately [4-5]. After that, the pH of the solution was reduced by adding acetic acid solution (0.1 $molL^{-1}$) to obtain pH about 3 to 4. In addition, 3g NCC particles were added to the mixture. Then the flask was placed in an oil bath and heated to about 60-70°C for about 30 minutes. At the same time, the mixture was stirred at 500 rpm using a magnetic stirrer in the oil bath. After finishing the reaction, the solution was centrifuged at 4000 rpm. Finally, the product was poured into deionized water for 24h to remove any remaining physical absorption. The sample then went under several washes by deionized water several times. The cellulose sample freeze-dried and powder form of MNCC was collected.

2.2.3.(i) Visual illustration of the preparation of MNCC

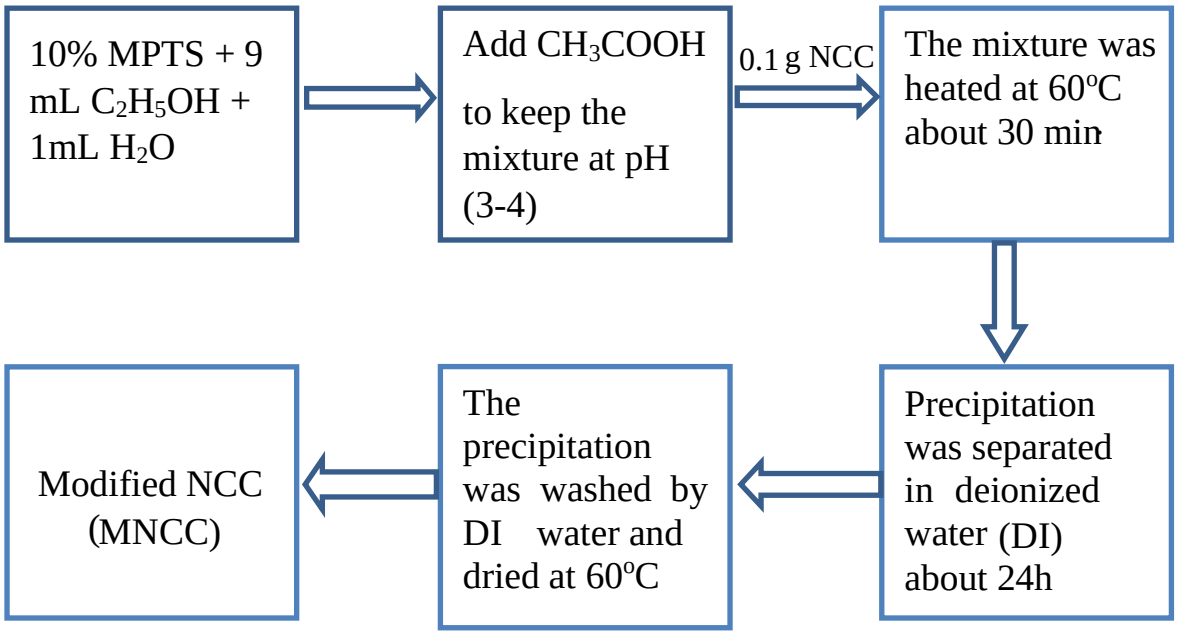

Fig. 2.2 The Route of synthesizing MNCC

2.2.5 Composition of different kinds of hydrogels

Table 2.1 Preparation recipe of PAA-Alg-MNCC-Fe^{3+} hydrogels by varying the concentration of Fe^{3+}

Sample codes	Acrylic acid (M)	MNCC (%)	Alginic acid (%)	KPS (mM)	TEMED (µL)	H_2O (mL)	$FeCl_3$ (%)
PAA-Alg-MNCC-Fe^{3+}-0.3%	4.00	1.00	1.00	0.1	20	4	0.3
PAA-Alg-MNCC-Fe^{3+}-0.45%	4.00	1.00	1.00	0.1	20	4	0.45
PAA-Alg-MNCC-Fe^{3+}- 0.6%	4.00	1.001	1.00	0.1	20	4	0.6
PAA-Alg-MNCC-Fe^{3+}- 0.75%	4.0	1.00	1.00	0.1	20	4	0.75
PAA-Alg	4.0	1.00	1.00	0.1	20	4	0.0

Table 2.2: Preparation recipe of PAA-Alg-MNCC-Fe^{3+} hydrogels by varying the concentration of MNCC cross-linker.

Sample codes	Acrylic acid (M)	MNCC (%)	Alginic acid (%)	KPS (mM)	TEMED (µL)	H_2O (mL)	$FeCl_3$ (%)
PAA-Alg-Fe^{3+} -MNCC 0.75%	4.00	0.75	1.00	0.1	20	4	0.1
PAA-Alg-Fe^{3+}-MNCC 1.00%	4.00	1.00	1.00	0.1	20	4	0.1
PAA-Alg-Fe^{3+} -MNCC 1.25%	4.00	1.25	1.00	0.1	20	4	0.1

2.3 Characterizations of synthesized materials:

2.3.1 FTIR spectroscopy analysis

First, the prepared sample was collected in a plastic test tube and freeze dried for about 2 hours. After drying the sample properly as a form of nice powder, it was then stored into the refrigerator at 5°C. Before running the FTIR spectra, the sample was ground and mixed (1:200) properly with pure KBr crystals. A mortar with a pestle was used to get a proper mixture**.** Next, a pellet was made by compressing the sample mixture with pressing tools with a pressure of about 8-10 tons. Finally, this prepared pellet is used for characterization by simply putting it under a designated sample chamber. Shimadzu IR spectrometer was used to collect the transmission mode of FTIR spectra. Spectra were obtained for each sample in the 400-4000 cm -1 range.

2.3.2 NMR analysis

This procedure used a solvent CDCl3 with an internal standard tetramethyl silane (TMS). To record ^{1}H-NMR spectra, Bruker BPX-400 spectrometer (400 MHz) was used. The coupling constant (j) and chemical shifts (δ) were measured in Hz and ppm, respectively. TMS peak and solvent peak at 7.28 ppm were recorded in chemical shift measurements. In the ^{1}H-NMR spectra s,d,t and q represent singlet, doublet, triplet, and quartet, respectively.

2.3.3 FE-SEM with EDS analysis

Using scanning electron microscopy (SEM), morphological studies were conducted. On a tiny piece of carbon strip, a drop of the diluted solution was applied, and it was then dried at 40 °C in a vacuum drier. The sample surface was coated with a thin coating of gold to increase electrical conductivity. The sample strip was then inserted into the SEM chamber for analysis. The device included a computer connection to capture the surface photos. Energy dispersive spectroscopy (EDS) was used to explain elementary maps and evaluate the qualitative elemental composition of the NCC and MNCC particles. [6-7]. To prepare the sample, it was dried carefully into the oven and coated with platinum to ensure the surface's conductivity. Finally, the sample was put into the sample chamber, and a SEM integrated with software was used to analyze it.

2.3.4 Elongation test

Tensile tests are carried out to determine the elongation, yield strength, and tensile strength of materials. At room temperature, this test was run by a universal testing machine (Instron, Model 3369, USA). At the preparation of this test, hydrogels were cut into rectangular shapes with measurements of 10 mm long and 4mm thick. The crosshead speed was fixed at 50 mm/min. Software attached to the machine helped to record the stress-strain curves. The equation used to measure the stress below $\sigma = F/\pi r^2$.

Here, r represents the initial radius of the specimen

F is the recorded load.

The strain (**ε**) was computed using the equation from the variation in the measured sample's length (l) from its original gauge length (lo). $\varepsilon = l / lo \times 100$

The initial slope of stress-strain curve was used to compute the initial modulus. The area of the stress-strain curve was integrated to determine the fracture toughness.

2.3.5 Compressive test

The compressive properties of hydrogels were measured on a UTM at room temperature. A 50 mm/min crosshead speed was used. To ensure consistency, each specimen was evaluated at least three times. The cylindrical hydrogel samples were made with 10-15 mm diameters and 4–8 mm thicknesses.

2.4 References

[1] Bondeson, D., Mathew, A., and Oksman, K., "Optimization of the isolation of nanocrystals from microcrystalline cellulose by acid hydrolysis", cellulose, vol. 13, pp. 171-180, 2006.

[2] Xiang, Q., Lee, Y. Y., Pettersson, P. O., & Torget, R., "Heterogeneous Aspects of Acid Hydrolysis of a-Cellulose", Applied Biochemistry and Biotechnology, vol. 705-108, pp. 505–514, 2003.

[3] Dong, X. M., Revol, J. F., & Gray, D., "Effect of microcrystalline preparation conditions on the formation of colloid crystals of cellulose", cellulose, vol. 5, pp. 19-32, 1998

[4] D. Schumacher, M. Wilhelm, and K. Rezwan, "Modified solution-Based freeze casting process of polysiloxanes to adjust pore morphology and surface functions of SiOC monoliths," Mater. Des., vol.160, pp.1295-1304, 2018.

[5] J. Jiang, W. Wang, H. Shen, J. Wang, and J. Cao, "Characterization of silica particles modified with γ-methacryloxypropyltrimethoxysilane," Appl. Surf. Sci., pvol. 397, pp. 104-111, 2017.

[6] Kian, L.; Saba, N.; Jawaid, M.; Alothman, O.; Fouad, H. Properties and characteristics of nanocrystalline cellulose isolated from olive fiber. Carbohydr. Polym., vol.241, pp. 116423, 2020.

[7] Abdul Rahman, N. H.; Chieng, B. W.; Ibrahim, N. A.; Abdul Rahman, N. Extraction and characterization of cellulose nanocrystals from tea leaf waste fibers. Polymers, vol. 9, pp. 588, 2017.

Chapter 3

Results and Discussion

3.1 Procedure to synthesize of PAA-Alg-MNCC-Fe^{3+} hydrogel

The method of synthesis of PAA-Alg-MNCC-Fe^{3+}hydrogel requires much attention and careful handling as the procedure is susceptible to temperature. First, AA, MNCC, Alg and 20µLTEMED were added in 3mLH_2Oin a vial. Then the mixture was magnetically stirred and sonicated for about 30 min. to get a well-dispersed mixture. At the same time, 0.004gm KPS and $FeCl_3$.6$H_2O$with different ration (1, 0.75, 0.5, 0.25% of monomer) were added into 1mL H_2O in a test tube. After that, both solutions were transferred into a different test tube and bubbled with nitrogen gas for 30 minutes to remove any dissolved oxygen. After finishing nitrogen bubbling, the KPS solution was slowly mixed with monomers. This mixing was done under several precautions, as the gel formed immediately due to excessive heat from the reaction. Thus it was conducted in an ice bath. Finally, the mixture was transformed into a glass mold. The hydrogel formation took place about 48h in 45-50ºC temperature.

3.2 The mechanism of Free-Radical polymerization

Free-radical polymerization follows a chain mechanism involving three key reactions: initiation, propagation, and termination.

Initiation begins with using thermally unstable compounds, such as potassium persulfate, which decompose under the influence of energy, often in the form of heat, to produce free radicals. These free radicals then attack the double bond of a reactive monomer, such as acrylic acid. Due to the pi electrons of the double bond being relatively distant from the nucleus, they are susceptible to attack by reactive species. When a free radical interacts with the pi electrons, a new pair of electrons is formed at a sigma level, while the other electron from the original pi electron pair is transferred to the other end of the acrylic acid molecule. This shift of the free-radical site occurs at the end of the acrylic acid molecule, allowing it to act as a free radical and attack another acrylic acid monomer.

Following initiation, the polymerization process enters the propagation stage. Here, the radical site in the first acrylic acid monomer unit attacks the double bond of a new monomer unit. This results in linking the second monomer unit to the first one and the transfer of the radical site from the initial monomer to the newly added monomer. The chain now possesses a radical site at its end carbon atom, enabling it to attack additional monomer units further. This step leads to continuous chain growth until termination occurs.

Termination represents the end of chain growth in the polymerization process. Termination can occur through two different mechanisms: coupling and disproportionation. Two growing polymer chains come into contact, and the radical sites on each chain form a bond, effectively neutralizing their reactivity. This bonding process results in the formation of a longer polymer chain. One growing polymer chain abstracts a hydrogen atom from another chain, forming two polymer chains. One chain ends up with a shorter length, while the other retains longer. This abstraction of a hydrogen atom stabilizes the radical sites on both chains, preventing further chain growth.

These steps of initiation, propagation, and termination govern the process of free-radical polymerization, enabling the formation of polymer chains from monomers.

3.3 Mechanism of free radical polymerization of AA

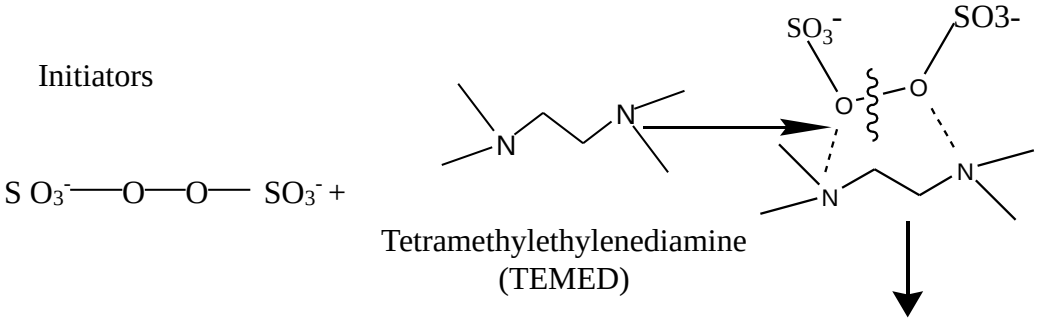

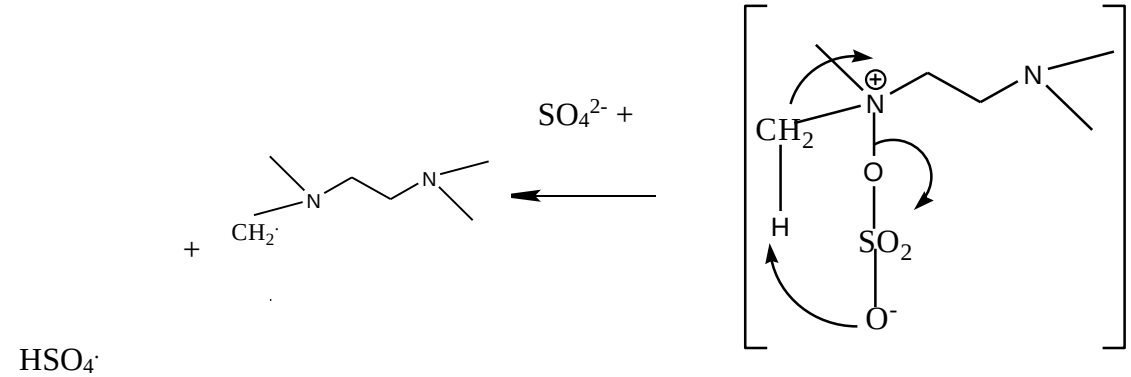

$HSO_4^{\cdot}$

H_2SO_4 +. OH $HSO_4^{\cdot} + H_2O$ R. =HSO4. **=. OH**

Initiation Propagation Termination

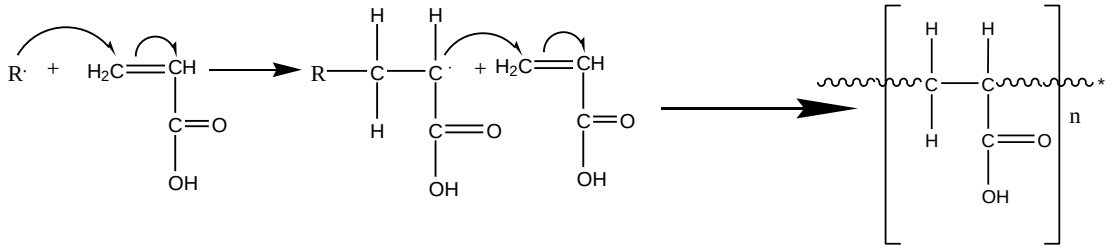

Acrylic acid (AA) Poly (acrylic acid)

chain

3.4 FT-IR characterization of NCC and MNCC to analyze functional groups

FTIR spectra of NCC and MNCC were conducted to investigate the probable functionalization process of the surface of NCC by MPTS. (fig 3.1). In this spectrum, the characteristic absorption band near 3440 cm^{-1} represents O-H bending vibrations in both MNCC and NCC spectra. Following modification with MPTS, the extra peak of carboxylic acid (C=O), and carbonyl groups (C=C) arise by the region at 1740cm^{-1} and 1630 $cm^{-1,}$ respectively. In the MNCC spectrum, some significant band had shown near 2957cm^{-1}, 2856 cm^{-1} due to C-H ($-CH_3$) stretching, C-H ($-CH_2$) stretching, respectively. Another absorption peak at 1100 cm^{-1} corresponds to Si-O-Si stretching vibration. Finally, it could be estimated that there are still a lot of unreacted O-H groups, as it shows a broad spectrum in the designated region of O-H. All these peaks and absorption bands indicate the successful grafting of functional groups of MPTS onto the surface of NCC.

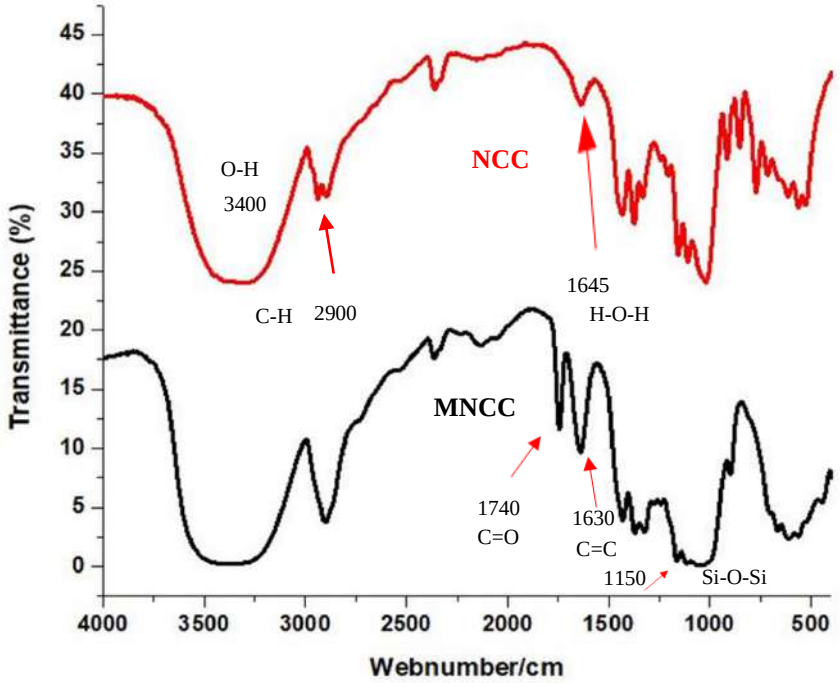

Fig. 3. 1: FT-IR spectrum of NCC and MNCC

Table 3. 1 FTIR analysis chart of NCC and MNCC

Wavenumbers (cm^{-1})	**Interpretation**
3440	O-H stretching vibration
2957	C-H ($-CH_3$) asymmetric stretching
2856	C-H($-CH_2$) symmetric stretching
1740	C=O Stretching vibration
1645	C=C Stretching vibration
1100	Si-O-Si stretching

3.5 Scanning Electron Microscopy (SEM) analysis of NCC and MNCC

Generally, SEM is used to study surface morphology and particle size, especially in nano scale. The SEM images of NCC and MNCC are presented in fig 3.2. These images were magnified about 50,000 to 100,000 times to analyze the surface of the samples. In SEM image of NCC, particles are estimated in nano size below 100 nm. This is because, after acid hydrolysis of microcrystalline cellulose, the micro fibers were fragmented into nano size. In both images, the particle size is shown below 100 nm. Nanoparticles in both samples are highly agglomerated, possibly due to the unreacted O-H group in the surface of NCC and MNCC which further form the O-H bond.

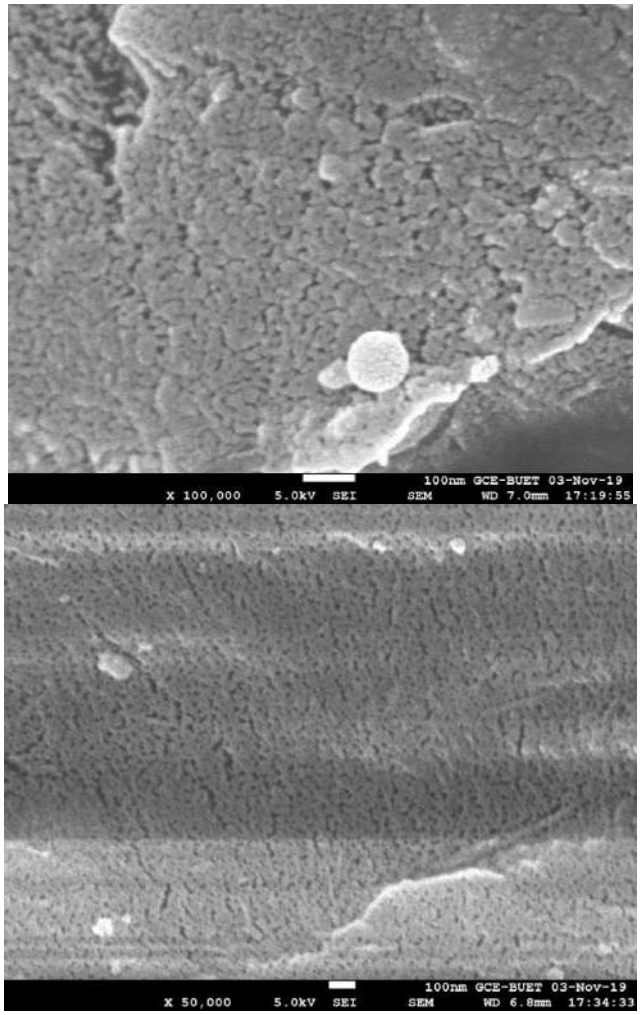

Fig. 3. 2 SEM images of a) NCC and b) MNCC

3.6 Energy-Dispersive X-ray Spectroscopy (EDS) analysis of NCC and MNCC

According to Table 3.2, the mass percentages of C, O in NCC are 59.33%, 40.67%, and the atomic ratio are 66.02%, 33.98%, respectively. It indicates the presence of carbon and oxygen atoms in the sample of NCC. On the other hand, table 3.3 shows the value of C, O, and Si in MNCC is 81.42% and 18.51%, 0.07%, respectively, whereas the atom percentages are 85.40%, 14.57%, and 0.03%. Here the change in the percentage of carbon and the presence of Si clearly shows the probable successful grafting of a silica-containing functional group in the surface of NCC.

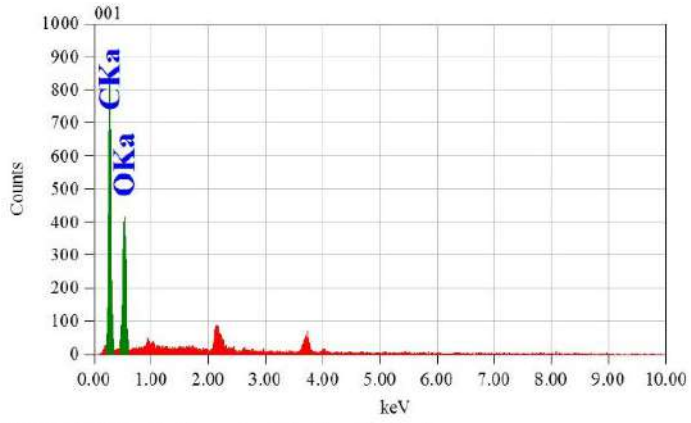

ZAF Method Standardless Quantitative Analysis
Fitting Coefficient : 0.1336

Element	(keV)	Mass%	Sigma	Atom%	Compound	Mass%	Cation
C K	0.277	59.33	0.43	66.02			
O K	0.525	40.67	0.72	33.98			
Total		100.00		100.00			

Fig. 3.3. EDS image of NCC

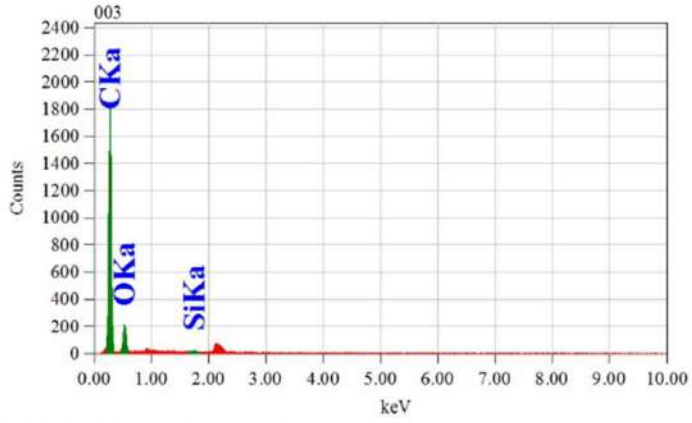

ZAF Method Standardless Quantitative Analysis
Fitting Coefficient : 0.1005

Element	(keV)	Mass%	Sigma	Atom%	Compound	Mass%	Cation
C K	0.277	81.42	0.08	85.40			
O K	0.525	18.51	0.18	14.57			
Si K*	1.739	0.07	0.05	0.03			
Total		100.00		100.00			

Fig. 3.4. EDS image of MNCC

Table 3. 2 EDS spectra of NCC

Atoms	**(KeV)**	**mass %**	**atom %**
C	0.277	59.33	66.02
O	0.525	40.67	33.98

Table 3. 3 EDS spectra of MNCC

Atoms	**(KeV)**	**mass %**	**atom %**
O	0.525	18.51	14.57
C	0.277	81.42	85.40
Si	1.739	0.07	0.03

3.7 Tensile test of PAA-Alg-MNCC-Fe^{3+}hydrogels

The mechanical properties of PAA-Alg-MNCC-Fe^{3+} hydrogels have been studied under uniaxial tension. Fig 3.5 and 3.6 represents the stress-strain curves of PAA-Alg-MNCC-Fe^{3+} hydrogel prepared by varying concentration of Fe3+ ion and the mechanical properties are summarized in Table 3.4. According to the data shown in fig 3.5 and 3.6, the maximum elongation and the corresponding fracture stress of PAA-Alg hydrogel are 1417% and 11kPa, respectively. Furthermore, PAA-Alg-MNCC-Fe^{3+} hydrogels are significantly improved by incorporating the Fe^{3+} in contrast to PAA-Alg hydrogel, fracture stress remarkably increases from 11 kPa to 57 kPa, when the Fe^{3+} concentration incorporate from 0.3 to 0.75 mol% against AA. When the Fe^{3+} concentration exceeds 0.45%, the fracture stress decreases marginally to 55 kPa, decreasing stretchability to 1153%. Similarly, the toughness of PAA-Alg-MNCC-Fe^{3+}-0.3% gels is 341.51 kJ/$m^{3,}$ though the PAA-Alg shows the highest toughness about 908 kJ/m3 (Fig 3.8).

Picture demonstrating that the hydrogels have high strength and toughness. When the concentration of Fe^{3+} ion exceeds 0.3%, the tensile strength and elongation at break of the PAA-Alg-MNCC-Fe^{3+} hydrogels decrease gradually with further increasing mass fractions of Fe^{3+}. Compared with the PAA-Alg hydrogel, the tensile strength of all the PAA-Alg-MNCC-Fe^{3+} hydrogel increases. This is due to various types of interactions. Such as, there is strong electrostatic and hydrogen bonding interaction between PAA, Alg polymer chain with MNCC, moreover the metal ligands coordination bond between -COO-/ Fe^{3+} ions.

However, the strain at break of PAA-Alg hydrogel is higher, about 1414.6%; we believe this is because of entanglement between two polymer chain (the PAA and the Alg chain). These chains can easily slide through each other. Thus, it increases the stretch ability of this hydrogel.

After introducing a cross-linker to PAA-Alg hydrogel, the stretchability is decreased gradually. As the ratio of Fe^{3+} Cross linker increased from 0.3% to higher, the stretchability had a significant demotion. It could be because the addition of cross-linkers is prohibited the movement of polymer chains, thus, the network gets regid. As the mass presentations of cross-linker increased, the rigidity and stretchability decreased.

Furthermore, the improvements in mechanical properties of PAA-Alg-MNCC-Fe^{3+} hydrogels originated from synergetic interactions of COO-/Fe^{3+} ionic coordination network [3] PAA covalent Network, high degree of network density and chain entanglements. When an external load is applied, the reversible physical ionic interactions act as "Sacrificial bonds" to dissipate energy [4-9] by rupture.

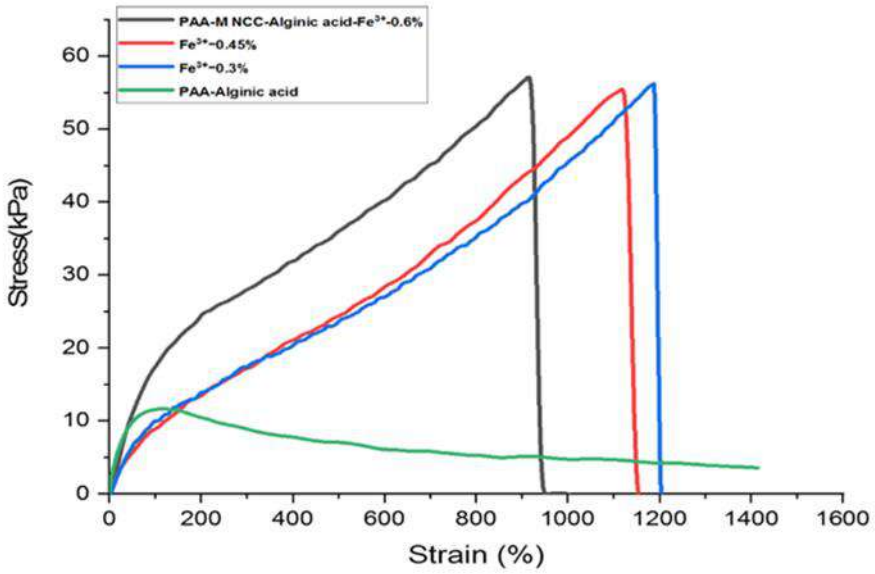

Fig. 3.5 Tensile test of PAA-Alg-MNCC-Fe^{3+} hydrogels

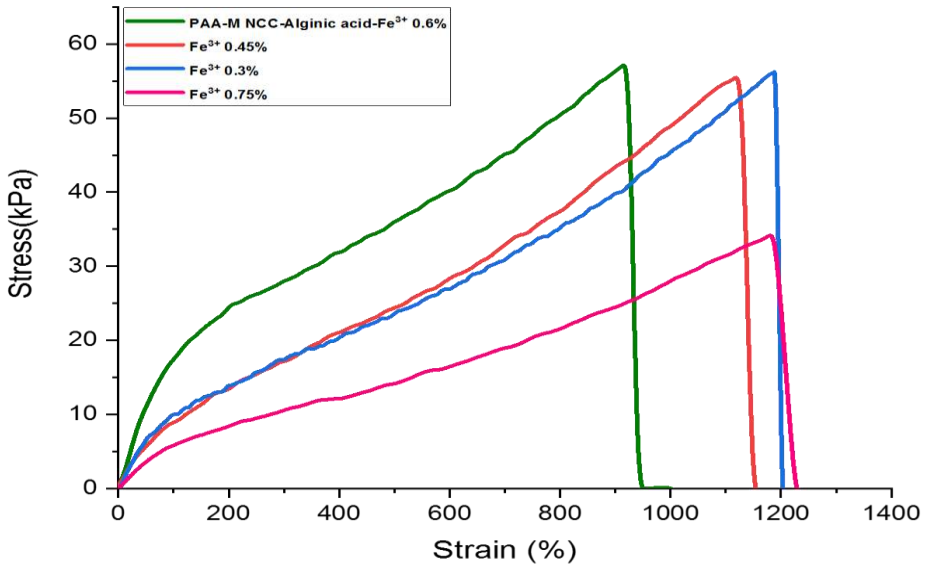

Fig. 3.6 PAA-Alg-MNCC-Fe^{3+} hydrogel's stress-strain curves with different compositions of Fe^{3+}

Table 3.4: Table for tensile properties of PAA-Alg-MNCC-Fe^{3+} hydrogels prepared by varying concentrators of Fe^{3+}

Sample code	**Toughness (kJ/m^3)**	**Tensile Strength (KPa)**	**Young Modulus (KPa)**	**Elongation at break (%)**
PAA-Alg	908	11.55	0.8	1414.6
PAA-Alg-MNCC-Fe^{3+}0.3%	341.51	56.2	4.7	1184.8
PAA-Alg-MNCC-Fe^{3+}0.45%	325.51	55.41	4.9	1115.9
PAA-Alg-MNCC-Fe^{3+}0.6%	61	31	0.91	138

3.8 Tensile test of PAA-Alg-MNCC-Fe^{3+} hydrogels prepared by varying concentrations of MNCC

Typical strain–stress curves of PAA-Alg-MNCC-Fe^{3+} for different weight (%) of cross-linker MNCC are given in Fig.3.7. Hydrogels with 0.75% MNCC cross-linker concentration against AA shows the highest tensile strength and elongation at break about 90 kPa and 1313 %, respectively. Furthermore, increasing the concentration of MNCC cross-linker to 1% decreases the tensile strength and elongation at break significantly, 40kPa and 980%, respectively. Increasing the concentration of MNCC cross-linker to 1.25% further decreases the tensile and elongation at break to 34 kPa and 561%, respectively**.** Here, hydrogels containing 0.75% MNCC, show high toughness, tensile strength at break by increasing the ratio to 1% to 1.25% MNCC, the mechanical properties are drastically decreased. This could be due to the addition of the MNCC cross-linker. The more MNCC cross-linker, the more rigid the polymer chain could get. The graph supports that by increasing the MNCC cross-linker to the polymer network, the mobility of the chain decreases, as polymer chains cannot slide to each other, the network becomes rigid. Thus, the stretchability, as well as elongation at break, reduce significantly. Thus, we successfully attributed the mechanical strength in PAA-Alg-MNCC-Fe^{3+} hydrogels to the following two aspects. Firstly, the improvement in mechanical properties of the following hydrogels is due to the addition of the well-dispersed MNCC cross-linker, considered a well-known typical strategy to reinforce polymeric composites in previous literature [1-2]. Secondly, the physical and covalent interaction between the polymer chain and well-dispersed cross-linker MNCC with PAA matrixes gives the polymer chains much freedom to dissipate energy under applied stress. Moreover, the dual ionic coordination bonds derived from Fe^{3+} and carboxylic groups of PAA chains and the carboxylated MNCC cross-linker surface act as a secondary crosslinking network, eventually improving mechanical performance.

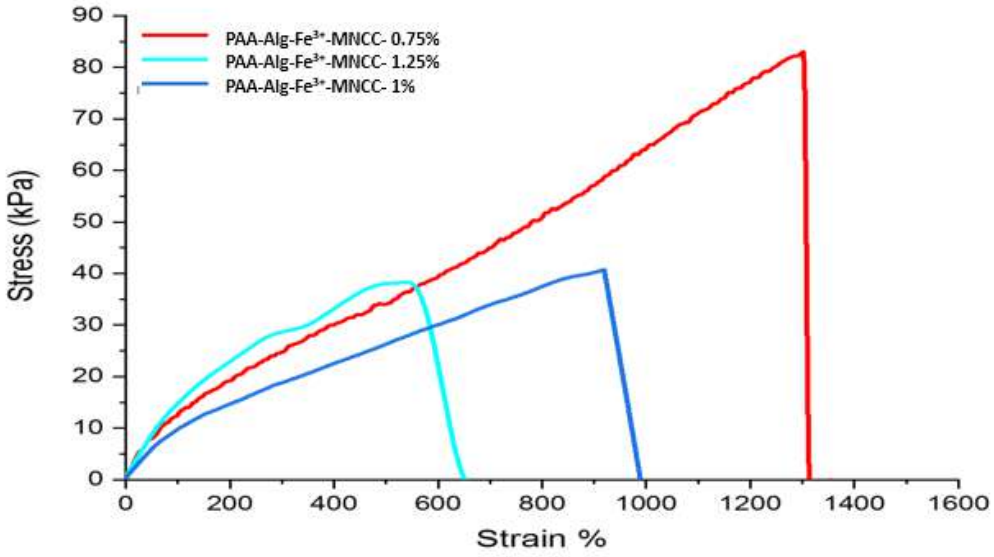

Fig. 3.7 PAA-Alg-MNCC-Fe^{3+}hydrogel's stress-strain curves with different compositions of MNCC

Table 3. 5 Tensile properties of PAA-Alg-MNCC-Fe^{3+} hydrogels by varying concentrations of MNCC

Sample code	**Toughness (kJ/m^3)**	**Tensile Strength (KPa)**	**Young Modulus (KPa)**	**Elongation at break (%)**
PAA-Alg-Fe^{3+} - MNCC-0.75%	589	90	6.8	1313
PAA-Alg-Fe^{3+}- MNCC-01.25%	188	34	7.6	561
PAA-Alg-Fe^{3+}- MNCC-0.1%	151	40	4.5	980

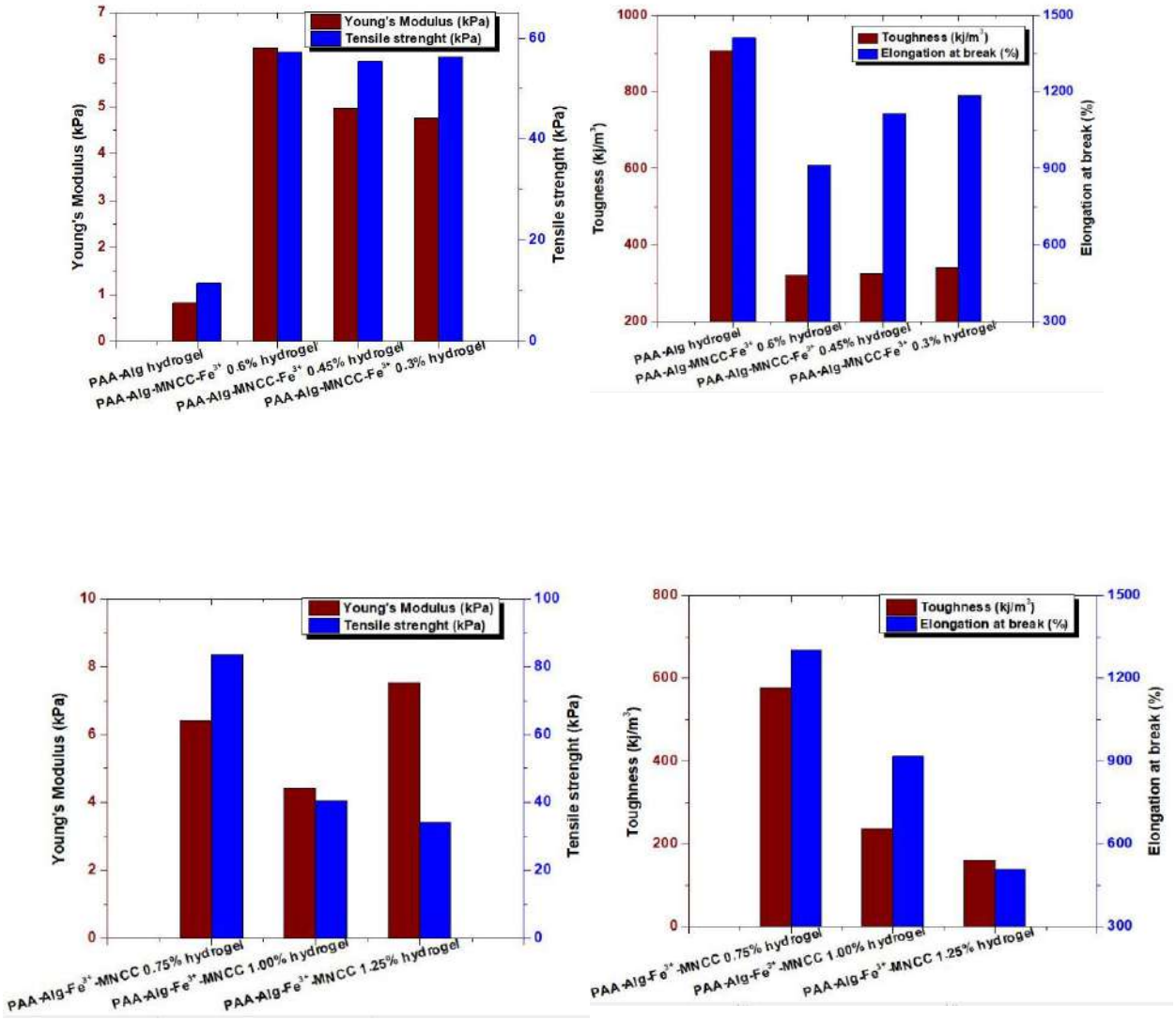

Fig. 3.8 Corresponding toughness and energy dissipation of PAA-Alg-MNCC-Fe^{3+} hydrogel varying the concentration of Fe^{3+} and MNCC cross-linker.

3.9 Photographs of PAA-Alg-MNCC-Fe^{3+} hydrogel during analysis of stress-strain curves under uniaxial tensile deformation

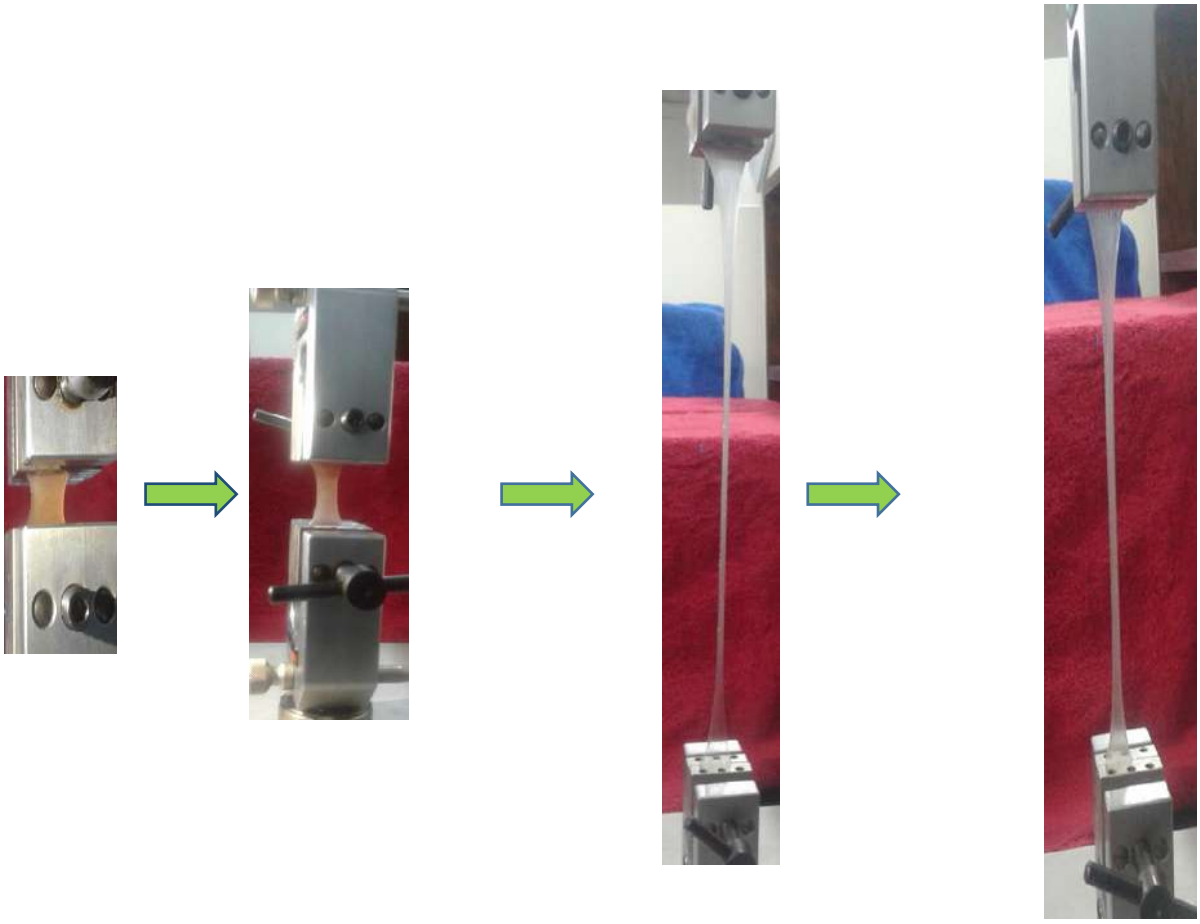

Initial **Final**

Fig. 3.9 Picture of PAA-Alg-MNCC-Fe^{3+} hydrogels while analyzing stress-strain curves under uniaxial tension.

3.10 Visual representations of self-healable PAA-Alg-MNCC-Fe^{3+} hydrogel

Original

After cutting

Healing

Stretching (after healing)

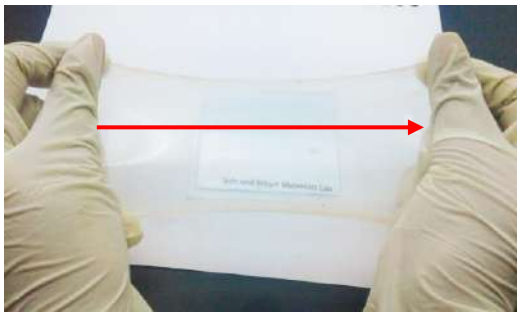

Extremely stretchable even after healing

Firstly, the samples were cut into two parts and placed at room temperature for 48h. The gel was healed without any external stimulation. Finally, the hydrogel healed and showed extreme stretchability. Self- healing strategy of this gel might be lies in the concepts of sacrificial bonds and energy dissipation mechanisms [10-11]. Based on the energy dissipation theory [12-15], the gels consist of two types of bonds. Firstly, the covalent bond results in permanent crosslinking and gives integrity to the hydrogel. Secondly, noncovalent bond such as hydrogen bond [16], metal-ligand coordination bonds [17] etc., can easily break and reform again. Thus, the reversible nature results in self-healing capacity in the hydrogel. However, once the covalent networks are ruptured, they cannot be reformed, and the damage is irreversible. [18]

One of the specific dynamic noncovalent bonds that give rise to self-healing is the metal−ligand coordination bond. Metal-ligand interactions within hydrogels can reversibly dissociate and associate rapidly [19]. These interactions have been harnessed as physical crosslinks to create high-strength hydrogels due to their efficient energy dissipation and quick recovery properties. Additionally, cellulose nanoparticles, abundant naturally occurring polysaccharides with a native crystalline structure, have gained immense interest as environmentally friendly reinforcing particles. Their modifiability, renewability, biodegradability, and excellent mechanical properties make them attractive for various applications [20-22]. NCC with numerous carboxyl groups along the backbone chains are selectively incorporated into elastomers. This inclusion expands the range of raw materials available for producing components and facilitates the formation of noncovalent bonds acting as sacrificial bonds within transient networks, thereby enabling the investigation of the energy dissipation mechanism [25]. Initially, MNCC forms a primary crosslinking network through hydrogen bonding with PAA chains. Subsequently, a secondary crosslinking network is introduced via dual ionic coordination bonds between Fe^{3+} ions and the carboxylic groups from PAA and carboxylated NCC [23-24]. This dual-network structure leads to tough gels, analogous to traditional hydrogels, where strong bonds create the primary network and weak bonds form a sacrificial network. However, in these physical gels, coordination bonds act as strong bonds, maintaining the primary structure, while hydrogen bonds serve as weak bonds forming the sacrificial network. What sets these hydrogels apart is that the coordination bonds, unlike in other hydrogels where they act as weak bonds, play the role of strong bonds in the current system. Nevertheless, they retain their dynamic nature, serving as sacrificial bonds [26] to dissipate energy after hydrogen bond rupture. This unique combination of high toughness, fast self-recovery, and significant self-healing properties after deformation or damage makes these hydrogels particularly noteworthy.

3.11 References

[1] Hore,M.J.A.; Composto,R.J.Functional Polymer Nanocomposites Enhanced by Nanorods. Macromoleculesvol,vol. 47,pp. 875−887, 2014.

[2] Yang, J.; Xu, F. Synergistic Reinforcing Mechanisms in Cellulose Nanofibrils Composite Hydrogels: Interfacial Dynamics, Energy Dissipation, and Damage Resistance. Biomacromolecules, vol. 18, pp. 2623−2632, 2017.

[3] Chen, W., Bu, Y., Li, D., Liu, C., Chen, G., Wan, X., & Li, N. High-strength, tough, andself-healing hydrogel based on carboxymethyl cellulose. Cellulose,vol. 27(2),pp.853–865, 2019.

[4] Barthelat, F.; Yin, Z.; Buehler, M. J. Structure and Mechanics of Interfaces in Biological Materials. Nat. Rev. Mater., vol.1, pp. 16007, 2016.

[5] Pilate, G.; Chabbert, B.; Cathala, B.; Yoshinaga, A.; Leple, J.-C.;´ Laurans, F.; Lapierre, C.; Ruel, K. Lignification and Tension Wood. C. R. Biol, vol.327, pp. 889−901, 2004.

[6] Altaner, C. M.; Jarvis, M. C. Modelling Polymer Interactions of the' Molecular Velcro' Type in Wood under Mechanical Stress. J. Theor. Biol, vol.253, pp. 434−445, 2008.

[7] Martin-Martinez, F. J.; Jin, K.; Lopez Barreiro, D.; Buehler, M.´ J. The Rise of Hierarchical Nanostructured Materials from Renewable Sources: Learning from Nature. ACS Nano vol.12, pp.7425−7433, 2018.

[8] Jin, K.; Qin, Z.; Buehler, M. J. Molecular Deformation Mechanisms of the Wood Cell Wall Material. J. Mech. Behav. Biomed. Mater. vol .42, pp.198−206, 2015.

[9] Shao, C., Chang, H., Wang, M., Xu, F., & Yang, J.High-strength, tough, and self-healing nanocomposite physical hydrogels based on the synergistic effects of dynamic hydrogen bond and dual coordination bonds. ACS Appl

Mater Int vol. 34(9), pp. 28305–28318, 2019.

[10] Luo F, Sun TL, Nakajima T, Kurokawa T, Zhao Y, Sato K, Ihsan AB, Li X, Guo H, Gong JP. Oppositely charged polyelectrolytes form tough, self-healing, and rebuildable hydrogels. Adv Mater, vol.17(27), pp. 2722–2727, 2025.

[11] Wang S, Guo G, Lu X, Ji S, Tan G, Gao L. A facile soaking strategy towards simultaneously enhanced conductivity and toughness of self-healing composite hydrogels through constructing multiple noncovalent interactions. ACS Appl Mater Int, vol. 22(10), pp. 19133–19142, 2018.

[12] Wang S, Guo G, Lu X, Ji S, Tan G, Gao L A facile soaking strategy towards simultaneously enhanced conductivity and toughness of self-healing composite hydrogels through constructing multiple noncovalent interactions. ACS Appl Mater Intol. 22(10), pp. 19133–19142, 2018.

[13] Li N, Chen G, Chen W, Huang J, Tian J, Wan X, He M, Zhang H Multivalent cations-triggered rapid shape memory sodium carboxymethyl cellulose/polyacrylamide hydrogels with tunable mechanical strength. Carbohyd Polym, vol.178, pp,159–165, 2017.

[14] Li N, Chen W, Chen G, Tian J Rapid shape memory TEMPO-oxidized cellulose nanofibers/polyacrylamide/ gelatin hydrogels with enhanced mechanical strength. Carbohyd Polym vol. 171, pp. 77–84, 2017.

[15] Li X, Zhao Y, Li D, Zhang G, Long S, Wang H Hybrid dual crosslinked polyacrylic acid hydrogels with ultrahigh mechanical strength, toughness and 63, 2017.

[16] Wei, Z.; He, J.; Liang, T.; Oh, H.; Athas, J.; Tong, Z.; Wang, C.; Nie, Z. Autonomous Self-Healing of Poly (acrylic acid) Hydrogels Induced by the Migration of Ferric Ions. Polym. Chem., vol. 4, pp. 4601− 4605. 2013.

[17] Rao, Y. L.; Chortos, A.; Pfattner, R.; Lissel, F.; Chiu, Y. C.; Feig, V.; Xu, J.; Kurosawa, T.; Gu, X.; Wang, C.; He, M.; Chung, J. W.; Bao, Z. Stretchable Self-Healing Polymeric Dielectrics Crosslinked through Metal-Ligand Coordination. J. Am. Chem. Soc. 2016, 138, 6020−6027.

[18] Chen, Q.; Zhu, L.; Chen, H.; Yan, H. L.; Huang, L. N.; Yang, J.; Zheng, J. A Novel Design Strategy for Fully Physically Linked Double Network Hydrogels with Tough, Fatigue Resistant, and Self-Healing Properties. Adv. Funct. Mater. 2015, 25, 1598−1607.

[19] Yang, J.; Xu, F.; Han, C. R. Metal Ion Mediated Cellulose Nanofibrils Transient Network in Covalently Crosslinked Hydrogels: Mechanistic Insight into Morphology and Dynamics. Biomacromolecules, vol. 18, pp. 1019−1028, 2017.

[20] Moon, R. J.; Martini, A.; Nairn, J.; Simonsen, J.; Youngblood, J. Cellulose Nanomaterials Review: Structure, Properties and Nanocomposites. Chem. Soc. Rev, vol. 40, pp. 3941−3994, 2011.

[21] Habibi, Y.; Lucia, L. A.; Rojas, O. J. Cellulose Nanocrystals: Chemistry, Self-Assembly, and Applications. Chem. Rev, vol. 110, pp. 3479−3500, 2010.

[22] Klemm, D.; Kramer, F.; Moritz, S.; Lindström, T.; Ankerfors, M.; Gray, D.; Dorris, A. Nanocelluloses: a New Family of NatureBased Materials. Angew. Chem., Int. Ed, vol. 50, pp. 5438−5466, 2011.

[23] Farhadnejad H, Mortazavi SA, Erfan M, Darbasizadeh B, Motasadizadeh H, Fatahi Y. Facile preparation and characterization of pH sensitive Mt/CMC nanocomposite hydrogel beads for propranolol-controlled release. Int J Biol Macromol vol. 111, pp. 696–705, 2018.

[24] Hossieni-Aghdama SJ, Foroughi-Nia B, Zare-Akbari Z, Mojarad-Jabali S, Motasadizadeh H, Farhadnejad H. Facile fabrication and characterization of a novel oral pHSensitive drug delivery system based on CMC hydrogel and HNT-AT nanohybrid. Int J Biol Macromol, vol. 107, pp. 2436–2449, 2018.

[25] Yang, J.; Xu, F. Synergistic Reinforcing Mechanisms in Cellulose Nanofibrils Composite Hydrogels: Interfacial Dynamics, Energy Dissipation, and Damage Resistance. Biomacromolecules, vol.18, pp. 2623−2632, 2017.

[26] Lin, P., Ma, S., Wang, X., & Zhou, F. Molecularly Engineered Dual-Crosslinked Hydrogel with Ultrahigh Mechanical Strength, Toughness, and Good Self-Recovery. Advanced Materials, vol. 27(12), pp.2054–2059, 2015.

Chapter 4
Conclusion

Conclusion

Biological soft tissues show similarities with hydrogel in terms of softness as well as strength under stress with hydrogels. Another specific characteristic of soft tissues is self-healing ability, which also was proved to be fabricated into hydrogel. This research aimed to incorporate special features such as self-healing capability and mechanical strength into hydrogel using a modified cellulose cross-linker. To prepare the hydrogel, NCC are successfully prepared by acid hydrolysis of microcrystalline cellulose, which was further functionalized with a silane-coupling agent**,**3-Methacryloxypropyltrimethoxysilane (MPTS). That Modified cellulose cross-linker was used as cross-linker to the hydrogel, which helped improve the gel's mechanical properties. FE-SEM, EDS, FT-IR analysis confirmed modification of NCC.FE-SEM micrographs of NCC and MNCC ensure the presence of intermolecular hydrogen bonds. Furthermore, NCC and natural polymer Alg were used to incorporate the biocompatible, biodegradable, nontoxic properties into the designed hydrogel. $FeCl_3.6H_2O$ was used to expect the straightforward ionic-crosslinking strategy, which had been used as an established material to incorporate self-healing properties.PAA-Alg-MNCC-Fe^{3+}hydrogels were prepared successfully by varying the concentration of Fe^{3+} and MNCC cross linkers by forming covalent and noncovalent bonds between the MNCC, Alg, Fe^{3+}, and AA polymer chain through *in-situ* free-radical polymerization. The PAA-MNCC-Alg-Fe^{3+} crosslinked hydrogel shows excellent toughness and elongation at break than the PAA-Alg hydrogel cross-linker containing hydrogel. Compared to PAA-Alg hydrogels, the addition of Fe3+ greatly enhances PAA-Alg-MNCC-Fe3+ hydrogels, and MNCC cross linker where the fracture stress noticeably rises from 11 kPa to 57 kPa when the concentration of Fe^{3+} is added from 0.3 to 0.75 mol% vs AA. The maximum tensile strength and elongation at break are shown by hydrogels with 0.75% MNCC cross-linker concentration compared to AA, measuring around 90 kPa and1313%, respectively. The PAA-Alg-MNCC-Fe^{3+} hydrogels showed excellent self-healing property, which is highly stretchable after damage within 24h recovery time where any external stimulation such as pH or temperature was not needed.

Finally, there is still scope to further research on this topic using various types of natural polymers such as hyaluronic acid and fulvic acid. This natural polymer will help produce biodegradable and biocompatible hydrogel with designated characteristics.

Attended Conference, Awards and Achievements

Conference Participation

- Conference on Environmental Solutions for Sustainable Development: Towards Developed Bangladesh (CESSD 2019) Organized by the Department of Chemistry, University of Dhaka on 27-28 November 2019.

- Symposium on Prospects and Future of STEM program in Bangladesh Organized by Bangladesh STEM Society on 2July 202019.

- International Conference on Recent Advance Chemistry (ICRAC 2020) Organized by the Department of Chemistry, Jagannath University, 7-8 February 2020.

ACHIEVEMENTS and AWARDS

- Awarded the prestigious Dr. Jaman Fellowship in 2019 by holding 2nd merit position at the Department of Chemistry BUET.

- Awarded the renowned National Science and Technology Fellowship (NST) 2018-19 by performing outstanding research work.

- Get recruited as a Teaching Assistantships (TA) | October 18 – April 19.

- Won the Championship in a fast-paced research competition Three Minute Thesis (3MT) organized by the Department of Chemistry BUET through zoom platform and judged by the expert panel from The University of Queensland and James Cook University, Australia, held on 7January 72021.

TRAININGS, WORKSHOPS and SEMINARS

- Seminar on 'Start up Chapter 2' Organized by the ICT Division in BUET.

Workshop on 'Introduction to Gaussian & Drug Discovery' Organized by the of

Chemistry, BUET on 1February 152020.

- Industrial visited to KAFOCO, DAP, CUFL and UGSFL Organized by the Department of Chemistry, BUET on 14-16 April 2019.

- Lab visits to CARS, BCSIR and BAEC Organized by the Department of Chemistry, BUET, on 6-9 April 2019.